Frequency-Comb Spectrum of Periodic-Patterned Signals

Johannes L. Steinmann,[1,*] Edmund Blomley,[2] Miriam Brosi,[1] Erik Bründermann,[2] Michele Caselle,[3]
Jeffrey L. Hesler,[4] Nicole Hiller,[2] Benjamin Kehrer,[1] Yves-Laurent Mathis,[2] Michael J. Nasse,[2] Juliane Raasch,[5]
Manuel Schedler,[1] Patrik Schönfeldt,[2] Marcel Schuh,[1] Markus Schwarz,[1] Michael Siegel,[5] Nigel Smale,[2]
Marc Weber,[3] and Anke-Susanne Müller[2]

[1]*Laboratory for Applications of Synchrotron Radiation, Karlsruhe Institute of Technology, 76131 Karlsruhe, Germany*
[2]*Institute for Beam Physics and Technology, Karlsruhe Institute of Technology, 76344 Eggenstein-Leopoldshafen, Germany*
[3]*Institute for Data Processing and Electronics, Karlsruhe Institute of Technology, 76344 Eggenstein-Leopoldshafen, Germany*
[4]*Virginia Diodes Inc., Charlottesville, Virginia 22902, USA*
[5]*Institute of Micro- und Nanoelectronic Systems, Karlsruhe Institute of Technology, 76187 Karlsruhe, Germany*
(Received 4 April 2016; published 20 October 2016)

Using arbitrary periodic pulse patterns we show the enhancement of specific frequencies in a frequency comb. The envelope of a regular frequency comb originates from equally spaced, identical pulses and mimics the single pulse spectrum. We investigated spectra originating from the periodic emission of pulse trains with gaps and individual pulse heights, which are commonly observed, for example, at high-repetition-rate free electron lasers, high power lasers, and synchrotrons. The ANKA synchrotron light source was filled with defined patterns of short electron bunches generating coherent synchrotron radiation in the terahertz range. We resolved the intensities of the frequency comb around 0.258 THz using the heterodyne mixing spectroscopy with a resolution of down to 1 Hz and provide a comprehensive theoretical description. Adjusting the electron's revolution frequency, a gapless spectrum can be recorded, improving the resolution by up to 7 and 5 orders of magnitude compared to FTIR and recent heterodyne measurements, respectively. The results imply avenues to optimize and increase the signal-to-noise ratio of specific frequencies in the emitted synchrotron radiation spectrum to enable novel ultrahigh resolution spectroscopy and metrology applications from the terahertz to the x-ray region.

Introduction.—Frequency combs are powerful tools for frequency metrology measurements spanning the range from radio frequencies (rfs) to more recent laser-based combs, encompassing nearly all spectral regions of the electromagnetic spectrum enabling, among other applications, high-resolution spectroscopy to study the rotational states of molecular gases and hyperfine structure lines of, e.g., ions, atoms, molecules, and radicals [1–4].

In general, frequency combs are generated by an almost infinite train of equally spaced short pulses. Some sources, however, have burstlike emissions separated by a gap between bursts of consecutive pulses. This can be the case for a high power laser that has to regenerate between emissions [5] or recent mode-locked laser systems that produce pulse bursts with a controllable number of pulses [6]. This applies also for accelerator based sources like free electron lasers [7] and especially synchrotron light sources with separated trains of electron bunches. In the past, the spectra of these time structures have been observed at pulsed bunch trains in linear accelerators [8] as well as synchrotrons [9] by interferometric methods. A separate case is machine-setting-independent phenomena like wake fields due to the shape of a given vacuum chamber, as studied in detail by Billinghurst *et al.* [10] [see Eq. (4)].

The observed peaks at specific frequencies have been found to depend on the filling pattern, the structure of pulse heights, and gaps. Recently, measurements showing the potential to exploit the discrete spectral lines of synchrotron radiation have been demonstrated with high resolution heterodyne methods [11]. The synchrotron frequency comb driven by the accelerating radio frequency and a second comb, both locked to the accelerator master oscillator, could enable dual-comb spectroscopy [12].

Here, we first provide a mathematical model to calculate the spectrum emitted by periodic sources in general and then support our findings with measurements at a synchrotron radiation facility where we systematically studied the effect of the filling pattern on the frequency-comb spectrum.

A detailed understanding of how the filling pattern influences the resulting spectrum is especially important for setups that can vary the parameters like pulse spacing and pulse height, synchrotron light sources, or setups that produce tunable electron trains in linear accelerators [13,14]. The results shown here can also be used for the direct analytic calculation of the spectral effects of manipulated pulse trains as used in laser-based experiments, e.g., by spectral self-imaging [15] or microwave modulation [16]. Additionally it has been shown that coupled-bunch instabilities in an accelerator can be damped by using special filling patterns [17].

Spectrum of repeating patterns.—The basis of a frequency comb is a signal $s_0(t)$ in the time domain that is

repeating after a period T_0. This can mathematically be described as an infinite series of Dirac delta pulses with distance T_0, convoluted with the signal of a single emission [18];

$$s(t) = \sum_{n=-\infty}^{\infty} s_0(t - nT_0) = \sum_{n=-\infty}^{\infty} \delta(t - nT_0) * s_0(t)$$
$$\equiv \text{III}_{T_0}(t) * s_0(t), \qquad (1)$$

where $*$ denotes convolution and III_{T_0} the Shah distribution [19].

In the simplest case the signal $s_0(t)$ consists of a single pulse $s_p(t)$. In the frequency domain, the convolution transforms into a multiplication. The Fourier transform of the Shah distribution is again a Shah distribution, leading to a discrete line spectrum at the revolution frequency harmonics $f_0 = 1/T_0$. The envelope is determined by the spectrum of the single pulse $S_p(f)$:

$$S(f) = \frac{1}{T_0} \sum_{p=-\infty}^{\infty} \delta(f - pf_0)S_p(f) = \frac{1}{T_0}\text{III}_{\frac{1}{T_0}}(f)S_p(f). \quad (2)$$

This is the known nature of the frequency comb. However, the signal s_0 may in general consist of a series of pulses with identical, normalized shape $s_p(t)$ and individual peak heights V_k,

$$s_0(t) = \sum_{k=1}^{h} V_k s_p(t - kT_p) = \underbrace{\left(\sum_{k=1}^{h} V_k \delta(t - kT_p) \right)}_{s_F(t)} * s_p(t).$$

$$\qquad (3)$$

It consists of a finite sum of h individual pulses separated by the pulse spacing time T_p and gap specified by $V_k = 0$. Note that V_k scales with the electric field of the pulse and not with the emitted power that is typically measured. The information of the position and height of the pulses is contained in the "filling pattern" function $s_F(t)$. The entire signal is then given by (cf. Fig. 1)
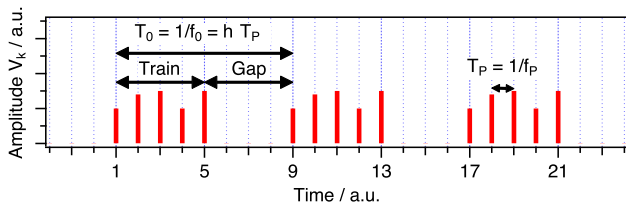
FIG. 1. Scheme of a signal pattern s_0 which repeats after the period time $T_0 = 1/f_0 = h\,T_p$. T_p denotes the time between consecutive pulses with individual height and h the number of slots. Here, the signal consists of a train of 5 pulses and a gap of 3 slots.

$$s(t) = \text{III}_{T_0}(t) * s_F(t) * s_p(t). \qquad (4)$$

Wake field effects due to the vacuum chamber (Billinghurst *et al.* [10]) could be incorporated in our formalism via the single pulse signal $s_p(t)$. The finite sum within the filling pattern s_F leads in the frequency domain to the discrete Fourier transformation (DFT) that is continuous and periodic with period $1/T_p = f_p$:

$$\text{DFT}\{s_F(t), f\} \equiv \sum_{k=1}^{h} V_k e^{-i2\pi f k T_p}. \qquad (5)$$

The Fourier transform of the entire signal is then given by

$$S(f) = \frac{1}{T_0}\text{III}_{\frac{1}{T_0}}(f) \times \text{DFT}\{s_F(t), f\} \times S_p(f). \quad (6)$$

It, $S(f)$, consists of the periodic DFT of the filling pattern, scaled by the spectrum of an individual pulse $S_p(f)$ and sampled by the Shah distribution. While in the time domain the convolution with the Shah distribution leads to a repetition of the one-turn signal after a period T_0, in the frequency domain, a multiplication with the Shah distribution leads to a discretization at multiples of $1/T_0 = f_0$. The main theoretical result is that the magnitude of the frequency comb peaks is determined and can easily be calculated by the DFT of s_F. In the following we investigate the effects of different filling patterns and give experimental evidence.

Influence of the filling pattern.—Since the energy in the time and frequency domain is identical, two pulses in a signal s_0 always result in the same overall power no matter where in the filling pattern they are located. However, different pulse spacing leads to changes in the shape of the spectrum due to the DFT of Eq. (6).

In Fig. 2, two scenarios are shown with a train of 5 consecutive pulses whose DFT leads to attenuated harmonics. The solid line results from 5 pulses with the same
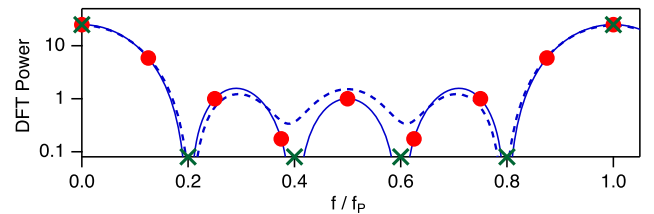
FIG. 2. $|\text{DFT}|^2$ of five consecutive pulses with distance T_p. According to Eq. (6), the DFT is sampled at discrete multiples of $f_0 = f_P/h$. Two exemplary cases are shown: Without a gap ($h = 5$) the DFT is sampled at multiples of $f_0 = f_P/5$ (green crosses). If a gap of three slots is added ($h = 8$) it is sampled at multiples of $f_0 = f_P/8$ (red dots). Solid line: all five pulses have the same height; dotted line: filling pattern as in Fig 1. Note how the uneven filling pattern leads to a sizable contribution at the zeros of the even filling pattern.

height. In this case the magnitude squared of the DFT has zeros at multiples of the repetition frequency f_P divided by the number of consecutive pulses h. In the complete spectrum [see Eq. (6)], the DFT is sampled only at the discrete harmonics of $f_0 = f_P/h$. For a total of 8 slots ($h = 8$), where a gap of 3 follows 5 pulses (positions as in Fig. 1), all harmonics have significant power according to the height of the DFT. On the other hand, the special case of $h = 5$ (without gap) leads to discrete harmonics at $f_0 = f_P/5$, corresponding to the zeros of the DFT. Consequently, only harmonics of f_P would be left. The case is different if the pulse height is not all the same. The dotted line in Fig. 2 depicts the $|\text{DFT}|^2$ if the height of the pulses is the one shown in Fig. 1. Here more harmonics of f_0 have significant value while the intensity at the f_P harmonics decreases accordingly (not visible on log scale).

The simplest case without enhancement is a single pulse. The power is equally distributed to all revolution frequency harmonics with a low over-all power drawback. The dc bin and all the f_P harmonics are the most intense frequencies, because the filling pattern signal $s_0(t)$ contains only positive values. These frequencies are maximized by an even filling pattern: every slot is filled with the same intensity. Every symmetry break of the time-domain signal leads to a power redistribution of the f_0 harmonics. While it's not possible to get enhancement at a single frequency, it is possible to enhance a pattern of specific frequencies. This can be done by superimposing a modulation with n periods onto the filling pattern, which will selectively enhance the f_0 harmonics at a distance $n \times f_0$ above and below every f_P harmonic.

Synchrotron radiation sources.—Most light sources are limited in simultaneous spectral coverage or bandwidth. However, synchrotron radiation sources, which are based on the emission of photons from relativistic electrons, are unique because they can provide powerful broadband light spanning several orders of the electromagnetic spectrum from the microwave region, via terahertz (THz), infrared and visible to the x-ray region, simultaneously. In the electron storage ring, which forms the core of a synchrotron light source, the repetition rate f_P of the pulses is the frequency of the accelerating field of the cavities f_{rf} determining the minimal pulse spacing. The period time is given by the revolution time of the circulating particles. The charge in the stored electron bunches constitutes the filling pattern. If the charged electrons are observed by pickup devices, the single pulse spectrum s_p corresponds usually to the detector response as the signal is much shorter than the resolution of the detector. If the emitted synchrotron light is observed directly, the single-pulse spectrum is given by the known synchrotron radiation spectrum [20].

Taking into account the enhancement of coherent synchrotron radiation (CSR)[21] with the form factor $F(f)$ and the number of electrons N_e in a bunch, the expected power of the synchrotron radiation is given by

$$|S(f)|^2 = \underbrace{\frac{1}{T_0} \text{III}_{\frac{1}{T_0}}(f)}_{f_0 \text{frequency comb}} \times \overbrace{\left| \sum_{k=1}^{h} V_k e^{-i2\pi f k T_{\text{rf}}} \right|^2}^{\text{filling pattern}}$$
$$\times \underbrace{[N_e + N_e(N_e - 1)F(f)]}_{\text{CSR enhancement}} \times \underbrace{|S_p(f)|^2}_{\text{SR spectrum}}. \quad (7)$$

A multibunch fill of a synchrotron light source can consist of several so-called trains with consecutively filled bunches that are separated by a gap to damp instabilities that could otherwise sum up and lead to beam loss.

The observation of this discrete spectrum is a standard tool for accelerator diagnostics [22–26] where the electric field induced into a pickup electrode is measured instead of the emitted synchrotron radiation. Since the bandwidths of these devices are limited and the focus is on beam instabilities which trigger additional frequencies, the influence of the filling pattern is most often neglected.

The discrete nature of synchrotron radiation could in the past hardly be resolved or exploited by experiments; therefore, synchrotron radiation in a storage ring is often treated in literature as a continuous spectrum (Ref. [27], p. 807).

However, the discrete frequencies and the influence of the filling pattern have been observed with very long interferometer arms [9] and recently by using THz heterodyne mixers that allow the resolution of single frequency peaks in the synchrotron spectrum [11]. The discrete frequency structure is due to the repeating emission in a storage ring and not limited to the THz range, but rather spans the entire synchrotron radiation spectrum up to the x rays. The comb purity and linewidth, however, will be disturbed by accelerator specific effects that scale with the frequency, such as coherent phase shifts or the occurrence of synchrotron frequency sidebands [28]. Low-alpha operation and active damping of synchrotron motion can minimize these sidebands. Coherent phase shifts can be reduced by using low particle energy, low bunch currents, or an even filling pattern. Controlling these effects maximizes the enhancement.

A yet unexploited advantage of the very broadband and intense synchrotron radiation in combination with frequency-comb measurements is that the electrons' revolution frequency is determined by the driving accelerating voltage. That leads to a very stable comb as well as the ability to easily change the comb spacing by adjusting the electrical master oscillator. At ANKA, changes of the rf frequency up to ± 10 kHz do not disturb the beam. Subsequently, above the 140th rf harmonic (≈ 70 GHz)

TABLE I. Parameters during measurements.

Electron beam energy	$E = 1.3$ GeV
Pulse (accelerating) frequency	$f_P = f_{\text{rf}} = 499.729$ MHz
Revolution frequency	$f_0 = 2.7159$ MHz
Number of slots	$h = f_P/f_0 = 184$
Local oscillator	LO $= 258$ GHz
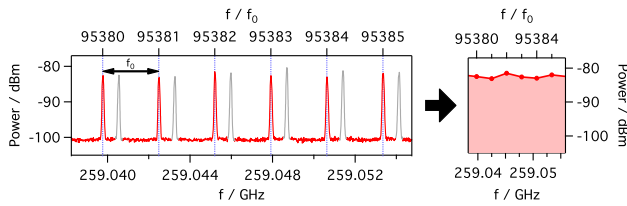
FIG. 3. Measured synchrotron radiation shows discrete harmonics of the revolution frequency at 259 GHz. The aliased LSB is shown in grey. For data reduction, only the intensity of each harmonic is used in the following, as shown on the right.

the frequency comb could be shifted by more than one frequency tooth, thus covering the whole frequency range without gaps, enabling ultrahigh resolution spectroscopy and metrology with better than 1 Hz.

In this Letter we expand on these previous experiments by systematically studying the influence of the filling pattern and comparing to our model.

Measurements.—Measurements have been performed at the IR1 beam line at the ANKA storage ring at the Karlsruhe Institute of Technology, Germany [29]. In a special short bunch length mode, the bunch length is reduced to a few picoseconds and CSR in the THz range can be observed [30,31]. Table I summarizes the parameters used for the measurements.

The synchrotron light is coupled out of the beam line at the diagnostic port and focussed by an off-axis paraboloid mirror and a horn antenna into a heterodyne Schottky mixer connected to a high bandwidth spectrum analyzer. By using the heterodyne receiver, the frequency resolution is determined by the spectrum analyzer, which is typically better by at least 6 orders of magnitude than the best interferometers in that frequency range. For further details of the experiment see

Ref. [32]. The used double-side-band mixer folds the frequencies above (upper side band, USB) and below (lower side band, LSB) the local oscillator (LO) into the same output. Because of the discrete spectrum of the synchrotron radiation, the folded frequencies of the USB and LSB can be separated, and artifacts and spurious signals identified and masked easily [32]. A measurement is presented in Fig. 3 where the frequency axis is only valid for the USB, the aliased contributions from the LSB are shown in grey. The discrete frequencies of the synchrotron radiation at multiples of f_0 can be seen. In the following data evaluation, only the peak maxima is taken into account.

Figure 4 presents data for different filling patterns. The displayed average noise level during the measurement was at -100 dBm. The filling pattern, shown in the right panel, has been recorded by time-correlated single-photon counting (TCSPC) that measures the intensity (i.e., the charge) of each electron bunch [33]. The initial filling pattern structure and different individual bunch currents resulted from the injection process of ANKA and instabilities, respectively. The preaccelerating booster formed one train consisting of 33 bunches, which was injected into the storage ring. Four trains from the booster filled up to 132 of the 184 possible slots. Then every second bunch was removed by the ANKA bunch-by-bunch feedback system [34]. This leads to additional peaks at multiples of 250 MHz separation. Even though the beam current decayed and half of the electrons in the storage ring were removed, the power at the specific 250 MHz harmonics increased by almost a factor of 10 with respect to the initial filling pattern. A similar result is observed when only every fourth bunch is kept and all others removed. Finally, a single bunch leads to a 2.71 MHz frequency comb whose harmonics have almost identical
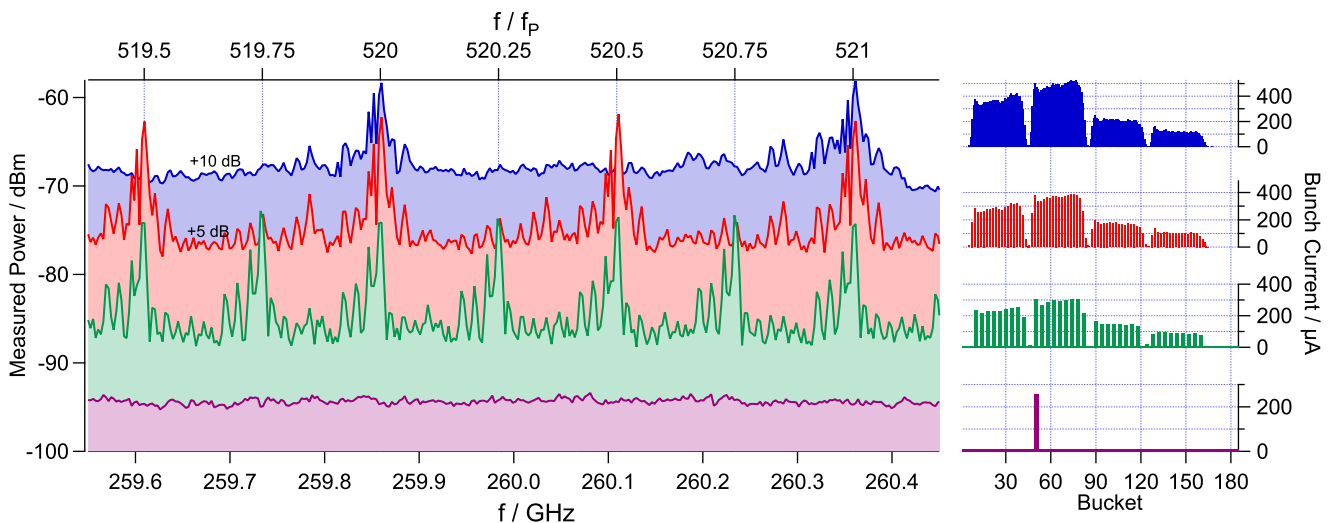
FIG. 4. Measured THz power spectrum at discrete multiples of the revolution frequency f_0 for different filling patterns. The right panel shows the corresponding filling pattern. The blue line corresponds to the initial filling pattern of 4 trains with 33 bunches each. For the red data set every second bunch was removed and for the green line only every fourth bunch is kept. For the purple line, only a single bunch is left leading to a 2.71 MHz frequency comb with almost equal power at all observed frequency teeth, differing only by 2 dB. For better visibility the red and blue data sets were shifted by $+5$ dB and $+10$ dB, respectively. The displayed average noise level was -100 dBm.

intensity around -94 dBm at a bunch current of 250 μA. That shows the potential to create specific enhanced frequencies by adjusting the filling pattern.

Summary.—We have developed a mathematical model to calculate the frequency-comb spectrum of emissions with gaps and different pulse amplitudes. We have demonstrated that the resulting frequency-comb spectrum is dependent on the DFT of the filling pattern. Consequently, the gap between trains and the length of the train lead to the leakage of power to the harmonics next to the main repetition frequency multiples. However, the difference in the pulse intensities is responsible for the overall power enhancement of revolution frequency harmonics. Furthermore, we have demonstrated that the harmonics of the revolution frequency that build up the synchrotron radiation spectrum in a storage ring, can be resolved even in the THz regime by heterodyne measurements. The actual filling pattern of the storage ring has a crucial influence on the observed spectrum and the amplification of specific frequencies. By adjusting the filling pattern, i.e., with a feedback system, enhanced frequencies can be created.

---

[*] johannes.steinmann@kit.edu

[1] T. Udem, R. Holzwarth, and T. W. Hänsch, Nature (London) **416**, 233 (2002).

[2] A. Schliesser, N. Picque, and T. W. Hänsch, Nat. Photonics **6**, 440 (2012).

[3] F. Keilmann, C. Gohle, and R. Holzwarth, Opt. Lett. **29**, 1542 (2004).

[4] S. Bartalini, L. Consolino, P. Cancio, P. De Natale, P. Bartolini, A. Taschin, M. De Pas, H. Beere, D. Ritchie, M. S. Vitiello, and R. Torre, Phys. Rev. X **4**, 021006 (2014).

[5] D. J. Den Hartog, N. Jiang, and W. R. Lempert, Rev. Sci. Instrum. **79**, 10E736 (2008).

[6] X. Li, S. Zhang, Y. Hao, and Z. Yang, Opt. Express **22**, 6699 (2014).

[7] H. H. Weits and D. Oepts, Phys. Rev. E **60**, 946 (1999).

[8] Y. Shibata, T. Takahashi, K. Ishi, F. Arai, H. Mishiro, T. Ohsaka, M. Ikezawa, Y. Kondo, S. Urasawa, T. Nakazato, R. Kato, S. Niwano, and M. Oyamada, Phys. Rev. A **44**, R3445 (1991).

[9] B. E. Billinghurst, J. C. Bergstrom, L. Dallin, M. de Jong, T. E. May, J. M. Vogt, and W. A. Wurtz, Phys. Rev. ST Accel. Beams **16**, 060702 (2013).

[10] B. E. Billinghurst, J. C. Bergstrom, C. Baribeau, T. Batten, L. Dallin, T. E. May, J. M. Vogt, W. A. Wurtz, R. Warnock, D. A. Bizzozero, and S. Kramer, Phys. Rev. Lett. **114**, 204801 (2015).

[11] S. Tammaro, O. Pirali, P. Roy, J. F. Lampin, G. Ducournau, A. Cuisset, F. Hindle, and G. Mouret, Nat. Commun. **6**, 7733 (2015).

[12] Y.-D. Hsieh, Y. Iyonaga, Y. Sakaguchi, S. Yokoyama, H. Inaba, K. Minoshima, F. Hindle, T. Araki, and T. Yasui, in *CLEO: 2014* (Optical Society of America, 2014), p. STh1N.2.

[13] P. Muggli, V. Yakimenko, M. Babzien, E. K. Kallos, and K. P. Kusche, Phys. Rev. Lett. **101**, 054801 (2008).

[14] Z. Zhang, L. Yan, Y. Du, Z. Zhou, X. Su, L. Zheng, D. Wang, Q. Tian, W. Wang, J. Shi, H. Chen, W. Huang, W. Gai, and C. Tang, Phys. Rev. Lett. **116**, 184801 (2016).

[15] R. Maram and J. Azaña, Opt. Express **21**, 28824 (2013).

[16] S.-C. Chan, G.-Q. Xia, and J.-M. Liu, Opt. Lett. **32**, 1917 (2007).

[17] S. Prabhakar, J. D. Fox, and D. Teytelman, Phys. Rev. Lett. **86**, 2022 (2001).

[18] Note that we use the engineering convention where lowercase functions refer to the time domain while upper case functions are in the frequency domain.

[19] R. Bracewell, *The Fourier Transform and its Applications*, 3rd ed. (McGraw-Hill, New York, 1999).

[20] J. Schwinger, Phys. Rev. **75**, 1912 (1949).

[21] C. J. Hirschmugl, M. Sagurton, and G. P. Williams, Phys. Rev. A **44**, 1316 (1991).

[22] J. M. Byrd, Bunched Beam Signals in Time and Frequency Domain, Proceedings of the Joint US, CERN, Japan, Russia School on Particle Accelerators, Montreux and CERN, Switzerland, 1998, (1998), pp. 233–262.

[23] R. Siemann, *AIP Conf. Proc.* 390, 3 (1997).

[24] A. Chao, *Physics of Collective Beam Instabilities in High Energy Accelerators* (Wiley, New York, 1993).

[25] S. Chattopadhyay, CERN Report No. 84-11 (1984).

[26] J. Laclare, CERN Report No. 84-03 (1987).

[27] H. Wiedemann, *Particle Accelerator Physics*, 3rd ed. (Springer, Berlin, 2007).

[28] J. L. Steinmann, E. Blomley, M. Brosi, E. Bründermann, M. Caselle, N. Hiller, B. Kehrer, A.-S. Müller, M. Schedler, M. Schuh, M. Schwarz, P. Schönfeldt, and M. Siegel, in *Proceedings, 7th International Particle Accelerator Conference* (IPAC, 2016), Vol. WEPOW015.

[29] Y.-L. Mathis, B. Gasharova, and D. Moss, J. Biol. Phys. **29**, 313 (2003).

[30] A.-S. Müller, I. Birkel, B. Gasharova, E. Huttel, R. Kubat, Y.-L. Mathis, D. Moss, W. Mexner, R. Rossmanith, M. Wuensch, P. Wesolowski, F. Perez, M. Pont, and C. Hirschmugl, in *Particle Accelerator Conference (PAC 05), Knoxville, Tennessee* (2005), p. 2518.

[31] A.-S. Müller, Rev. Accel. Sci. Techol. **03**, 165 (2010).

[32] J. L. Steinmann, M. Brosi, E. Bründermann, M. Caselle, E. Hertle, N. Hiller, B. Kehrer, A.-S. Müller, P. Schönfeldt, M. Schuh, P. Schütze, M. Schwarz, and J. Hesler, in *Proceedings of the IPAC'15, Richmond, Virginia, USA* (2015).

[33] B. Kehrer, P. Schütze, P. Schönfeldt, M. Holz, E. Hertle, N. Hiller, and A.-S. Müller, in *Proceedings of the IPAC'15, Richmond, Virginia, USA* (2015), Vol. MOPHA037.

[34] E. Hertle, N. Hiller, E. Huttel, B. Kehrer, A.-S. Müller, N. J. Smale, M. Höner, and D. Teytelman, in *Proceedings of IPAC'14, Dresden, Germany* (2014), Vol. TUPRI074.